THE ARCHIVE OF MECHANICAL ENGINEERING

Vol. XLIX 2002 Number 1

**Key words:** *panel methods, surface vorticity distribution, airfoil theory, low-speed aerodynamics*

*PIOTR STRZELCZYK*[*)]

# CALCULATION OF TWO-DIMENSIONAL VELOCITY DISTRIBUTION BY SURFACE VORTICITY METHOD

In the paper, the author presents a certain approach to interpretation of surface vorticity distribution on the airfoil surface, which leads to reduction of computational cost of surface vorticity distribution method (SVM). Some examples of the calculations are shown, and the results compared with solutions based on conformal mapping method as well as with experimental data. The calculations were done employing linear vortex distributions on each panel. The Neuman boundary condition was established at the collocation points. An unloaded trailing edge Kutta-Joukowski condition was applied in the present work. The interpretation of continuous vorticity distribution at the airfoil surface made it possible to reduce the number of panels on airfoil surface, and a satisfactory accuracy was maintained. In these circumstances one can do the calculations even by means of a programmable calculator.

## Nomenclature

| | |
|---|---|
| $a_{ij}$ | influence coefficient, |
| $b_j$ | element of right hand-side vector in the system of equations, |
| $N$ | number of boundary elements, |
| $r$ | Radius, |
| $u$ | component of velocity vector in $0x$ direction, |
| $\overline{v} = u - iw$ | complex velocity, here: $i = \sqrt{-1}$ , |
| $V_\infty$ | inflow velocity, |
| $w$ | component of velocity vector in $0z$ direction, |
| $x, z$ | coordinates of Cartesian coordinate system, |
| $y=x+iz$ | complex variable at $x0z$ plane, here: $i = \sqrt{-1}$ , |
| greek symbols: | |
| $\alpha$ | angle of attack, |

[*)] *Rzeszow University of Technology, ul. W. Pola 2, 35-959 Rzeszów, Poland; E-mail: piotstrz@prz.rzeszow.pl*

| | |
|---|---|
| $\beta$ | panel inclination angle, referred to $0x$ axis of global reference frame, |
| $\gamma$ | intensity of Vorticity, |
| $\eta = y_c - x \equiv re^{\Theta}$ | auxiliary complex coordinate at y-plane, |
| $\Theta$ | polar coordinate of complex variable $\eta$, |
| subscripts: | |
| $C$ | referred to collocation point, |
| $G$ | referred to global system of coordinates, |
| $L$ | referred to left-hand side value of circulation intensity on boundary element, |
| $n$ | normal component, |
| $P$ | referred to the endpoint of boundary element, |
| $R$ | referred to right-hand side value of circulation intensity on boundary element, |
| $t$ | tangential component. |

## 1. Introduction

The surface vorticity modelling (SVM) is one of the so-called panel or boundary element methods. The concept of the method was given by Martensen [10] in 1959. Many other investigators have developed SVM computational algorithms for the flow past the airfoil, employing various types of vorticity distributions. There were also different forms of boundary conditions, as well as Kutta-Joukowski conditions for trailing edge. The most common form of boundary condition is vanishing of normal velocity at collocation points, placed in the middle of each panel [3], [4], [5]. However, sometimes the internal condition of zero tangential velocity is applied [13], [15]. In some works, a panel methods based on stream function has been employed [2], [11]. Moreover, Babah [11] placed collocation point at the surface of the airfoil. In the method presented in [11], the author employs piecewise linear vorticity distribution. Stalewski [15] has developed method based on linear surface distribution of sources and vortices. In this method, a Dirichlet boundary condition has been applied. Sorko presented [13] a similar method, however, a condition of zero tangential velocity at the internal side of contour wa applied. The method has been applied for isolated airfoil as well as linear cascades.

Some authors, like Belotserkovskii [3], Xu and Yeung [17] have also investigated separated flow around the airfoil. The computational algorithm in both cases is based on distribution of discrete vortices on airfoil surface and free vortices shed from separation points. A much more simplified method for simulation of separated flows around bluff two dimensional bodies was given by Chiu [4]. The author makes use of linearly variable vorticity distribution, and a prescribed rigid wake. The wake is attached at the boundary layer separation points. An extensive review of some other two dimensional panel methods may

be found in the book by Katz and Plotkin [9].

In the present paper, the author employs an interpretation of surface vorticity distribution given by Martensen to obtain tangential (surface) velocity distribution over an airfoil. The similar approach was applied by Xu [16] for determination of velocity on airfoil. However, the method applied in [16] was based on piecewise constant vorticity distribution with boundary condition with zero tangential velocity at the internal surface. Moreover, tangential velocity has been calculated at the midpoints of boundary elements.

The present paper is restricted to the two dimensional problems only. However, the panel methods have wide range of applications for three dimensional cases. A review of this applications in aerodynamics and flight mechanics may be found in [7], [8], [9].

## 2. Outline of numerical procedure

Here we consider a method based on linear (trapezoidal) vortex distribution over each panel. Because vorticity distribution must be continuous over airfoil surface there is a need to establish the condition of equality the of values of vorticity at right-hand end of previous, and left-hand end of the current panel, respectively. This corresponds to continuous distribution of tangential velocity. Moreover, once vorticity distribution is calculated, the velocity at the panel corners is directly given. Note that this velocity is calculated *at the airfoil surface*. In the case of methods presented in [4], [5], [9] the velocity is calculated in the collocation points which lay inside or outside of the airfoil contour[1]. Let us denote the following angles and radii in local (panel) coordinate system (Fig. 1):

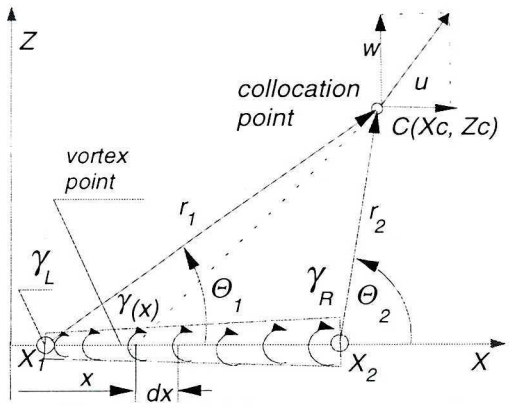


Fig. 1. Local systems of coordinates for linear vortex distribution

[1] That depends on local curvature of airfoil surface.

$$r_1 = \sqrt{(x_C - x_1)^2 + z_C^2}, \qquad r_2 = \sqrt{(x_C - x_2)^2 + z_C^2},$$
$$\Theta_1 = \operatorname{arc\,tg}\frac{z_C}{x_C - x_1}, \qquad \Theta_2 = \operatorname{arc\,tg}\frac{z_C}{x_C - x_2}. \tag{2.1}$$

Now, let vorticity distribution over individual panel be given as a linear function in panel coordinate system (Fig. 1.)

$$\gamma(x) = \gamma_L + \frac{\gamma_R - \gamma_L}{x_2 - x_1}(x - x_1). \tag{2.2}$$

To determine velocity field induced by linear vorticity distribution, it is convenient to decompose velocity distribution into constant and triangular part, as shown at Fig. 2.

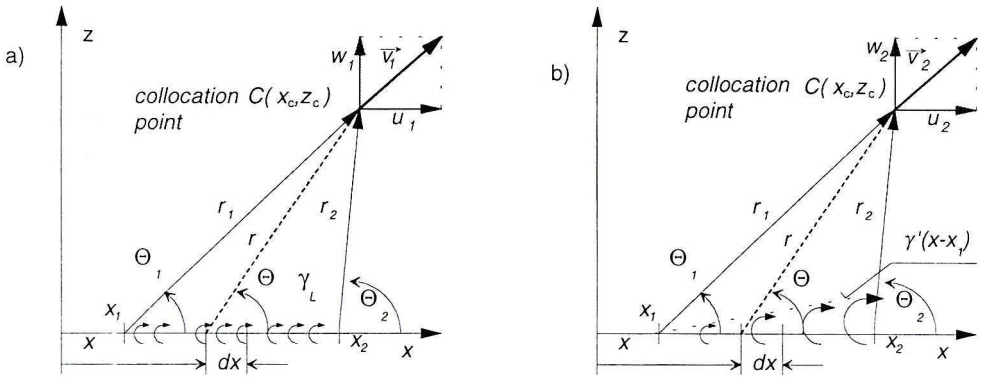


Fig. 2. Decomposition of linear vorticity distribution. Constant vorticity distribution (a) and triangular vorticity distribution (b)

Derivation of equations for the velocity components would be simplified by expressing of the induced velocity as a complex variable.
Let

$$\overline{v} = u - iw, \tag{2.3}$$

be a complex velocity at the complex plane: $y=x+ iz$.
Now, let us assume that vorticity is distributed along $x$ axis, as shown in Fig. 2a. The complex velocity generated by the constant vorticity distribution will be given by the expression:

$$\overline{v}_1 = i\frac{\gamma_L}{2\pi}\int_{x_1}^{x_2}\frac{dx}{y_c - x}. \tag{2.4}$$

Now, we introduce auxiliary variable $\eta$ defined as follows

$$\eta = y_c - x \equiv re^{i\Theta}, \tag{2.5}$$

after integration and substitution

$$\eta_1 = r_1 e^{i\Theta_1}; \qquad \eta_2 = r_2 e^{i\Theta_2}, \tag{2.6}$$

we get

$$\overline{v_1} = \frac{\gamma_L}{2\pi}\left[\Theta_2 - \Theta_1 - i\ln\frac{r_2}{r_1}\right]. \tag{2.7}$$

Hence, the components of the velocity generated by constant vorticity distribution $\gamma_L$ are:

$$u_1 = \frac{\gamma_L}{2\pi}(\Theta_2 - \Theta_1), \tag{2.8a}$$

$$w_1 = \frac{\gamma_L}{2\pi}\ln\frac{r_2}{r_1}. \tag{2.8b}$$

Now, let us consider triangular vorticity distribution (Fig. 2b)

$$\gamma(x) = \gamma'(x - x_1) \quad \text{for} \quad x \in \langle x_1; x_2 \rangle. \tag{2.9}$$

Where:

$$\gamma' = (\gamma_R - \gamma_L)/(x_2 - x_1). \tag{2.10}$$

Then complex velocity induced by vorticity distribution described by equation (2.9) is given by

$$\overline{v_2} = i\frac{\gamma'}{2\pi}\int_{x_1}^{x_2}\frac{(x - x_1)\,dx}{y_c - x}. \tag{2.11}$$

After substitution of an auxiliary variable $\eta$ into (2.11) and integration by parts we get

$$\overline{v_2} = i\frac{\gamma'}{2\pi}\left[\eta_2 - \eta_1 - y_c\ln\frac{\eta_2}{\eta_1} + x_1\ln\frac{\eta_2}{\eta_1}\right], \tag{2.12}$$

substituting (2.6) into (2.12) we get:

$$u_2 = \frac{\gamma'}{2\pi}\left[z_c\ln\frac{r_2}{r_1} + (x_c - x_1)(\Theta_2 - \Theta_1)\right], \tag{2.13a}$$

$$w_2 = \frac{\gamma'}{2\pi}\left[(x_c - x_1)\ln\frac{r_2}{r_1} - z_c(\Theta_2 - \Theta_1) + x_2 - x_1\right]. \tag{2.13b}$$

Now, the induced velocity may be expressed as a sum of the components (2.8) and (2.13):

$$\begin{aligned} u &= u_1 + u_2, \\ w &= w_1 + w_2. \end{aligned} \tag{2.14}$$

This allows us to decompose components of the induced velocities into parts dependent on the values of vorticity at the edges of the boundary element. Moreover, it is rational to put the origin of the panel coordinate system at the beginning of boundary element. This will lead to further simplification of the formulae for induced velocity, because $x_1 = 0$.

Now, substituting (2.10) into (2.13) and making use of (2.14) one may get:

$$u_L = \frac{\gamma_L}{2\pi}\left[\frac{z_C}{x_2}\ln\frac{r_1}{r_2} + \left(1 - \frac{x_C}{x_2}\right)(\Theta_2 - \Theta_1)\right], \tag{2.15a}$$

$$u_R = -\frac{\gamma_R}{2\pi}\left[\frac{z_C}{x_2}\ln\frac{r_1}{r_2} - \frac{x_C}{x_2}(\Theta_2 - \Theta_1)\right]. \tag{2.15b}$$

In the mid-point of the panel ("self-induction"):

$$u_L = \gamma_L/4, \qquad u_R = \gamma_R/4, \qquad u = (\gamma_L + \gamma_R)/4. \tag{2.15c}$$

For vertical component of induced velocity in the local (panel) coordinate system we have

$$w_L = -\frac{\gamma_L}{2\pi}\left[1 - \frac{z_C}{x_2}(\Theta_2 - \Theta_1) + \left(1 - \frac{x_C}{x_2}\right)\ln\frac{r_1}{r_2}\right], \tag{2.15d}$$

$$w_R = -\frac{\gamma_R}{2\pi}\left[\frac{x_C}{x_2}\ln\frac{r_1}{r_2} + \frac{z_C}{x_2}(\Theta_2 - \Theta_1) - 1\right], \tag{2.15e}$$

and self-induction of current panel:

$$w_L = -\gamma_L/2\pi, \qquad w_R = \gamma_R/2\pi, \qquad w = (\gamma_R - \gamma_L)/2\pi. \tag{2.15f}$$

The indices *"L"* and "R" denote that the velocity component in dependent on left end or right end value of vorticity distribution. Now, we may shortly describe computational algorithm.

Step 1: Grid generation

The airfoil is divided into $N$ panels by $N+1$ points $P$ with given coordinates. There, he points $P(1)$ and $P(N+1)$ correspond to the trailing edge point. Now, one should calculate $N$ collocation points C with coordinates:

$$\begin{aligned} x_{C\,j} &= \left(x_{P\,j} + x_{P\,j+1}\right)/2, \\ z_{C\,j} &= \left(z_{P\,j} + z_{P\,j+1}\right)/2, \end{aligned} \tag{2.16}$$

for j=*1*...*N*.

It is also necessary to know sine and cosine of angles between panel and direction of axis $OX_G$ in the global coordinate system:

$$\sin\beta_j = \frac{z_{P\,j+1} - z_{P\,j}}{\sqrt{\left(x_{P\,j+1} - x_{P\,j}\right)^2 + \left(z_{P\,j+1} - z_{P\,j}\right)^2}}, \tag{2.17}$$

$$\cos\beta_j = \frac{x_{P\,j+1} - x_{P\,j}}{\sqrt{\left(x_{P\,j+1} - x_{P(j)}\right)^2 + \left(z_{P\,j+1} - z_{P\,j}\right)^2}},$$

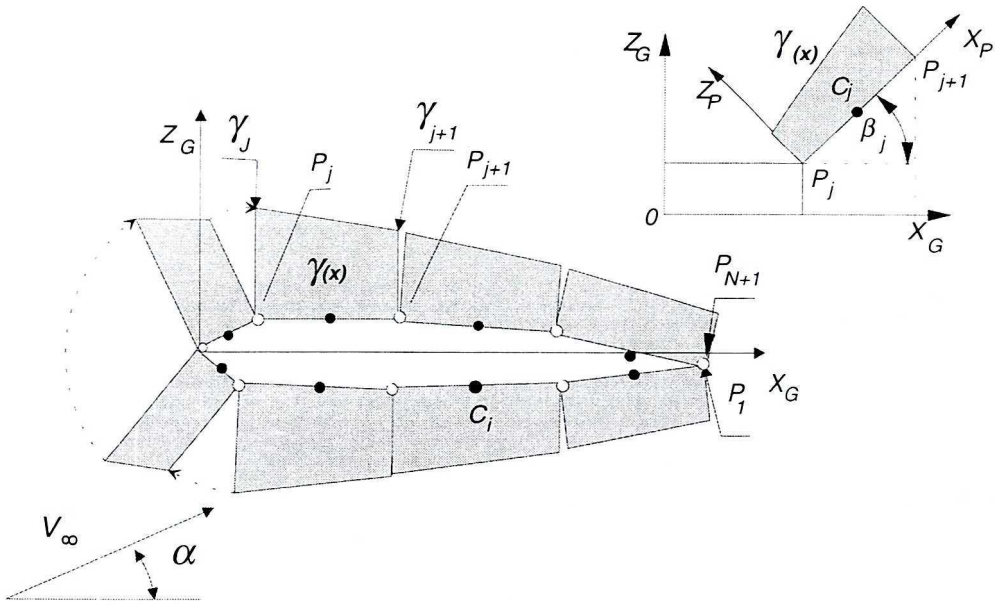


Fig. 3. Panel grid of an airfoil surface. Schematic

Step 2: Determination of influence coefficients

For each collocation point „*j*" one should calculate velocities induced by panel number „*i*". For this purpose there is a need to transform collocation point to the system of coordinates of currently considered panel:

$$\begin{cases} x_C^{(P)} = \left(x_{Cj} - x_{Pi}\right)\cos\beta_i + \left(z_{Cj} - z_{Pi}\right)\sin\beta_i, \\ z_C^{(P)} = \left(z_{Cj} - z_{Pi}\right)\cos\beta_i - \left(x_{Cj} - x_{Pi}\right)\sin\beta_i, \\ x_2 = \left(x_{Pi+1} - x_{Pi}\right)\cos\beta_i + \left(z_{Pi+1} - z_{Pi}\right)\sin\beta_i. \end{cases} \tag{2.18}$$

Then, one may calculate velocities induced by each boundary element in collocation point, and decompose the velocity into parts dependent on left and right value of vorticity strength:

$$\begin{aligned} u_{ij} &= u_{Lij}^{(1)}\,\gamma_i + u_{Rij}^{(1)}\,\gamma_{i+1}, \\ w_{ij} &= w_{Lij}^{(1)}\,\gamma_i + w_{Rij}^{(1)}\,\gamma_{i+1}. \end{aligned} \tag{2.19}$$

The upper index *"1"* denotes value of the velocity for unit strength of vorticity, $\gamma=1$.

Now after transformation to global coordinate system $0X_GZ_G$, we have:

$$\begin{aligned} u_{ij}^{(1)} &= u_{GLij}^{(1)}\gamma_i + u_{GRij}^{(1)}\gamma_{i+1}, \\ w_{ij}^{(1)} &= w_{GLij}^{(1)}\gamma_i + w_{GRij}^{(1)}\gamma_{i+1}, \end{aligned} \tag{2.20}$$

where „G" denotes global system of coordinates. The components of velocity induced by boundary element number $i$ at collocation point number $j$ for unit circulation strength $\gamma=1$ are equal:

$$\begin{aligned} u^{(1)}_{GL\,ij} &= u^{(1)}_{L\,ij}\cos\beta_i - w^{(1)}_{L\,ij}\sin\beta_i, \\ u^{(1)}_{GR\,ij} &= u^{(1)}_{R\,ij}\cos\beta_i - w^{(1)}_{R\,ij}\sin\beta_i, \\ w^{(1)}_{GL\,ij} &= u^{(1)}_{L\,ij}\sin\beta_i + w^{(1)}_{L\,ij}\cos\beta_i, \\ w^{(1)}_{GP\,ij} &= u^{(1)}_{R\,ij}\sin\beta_i + w^{(1)}_{R\,ij}\cos\beta_i. \end{aligned} \tag{2.21}$$

Making use of the above equations, one may write boundary condition at point $j$

$$\begin{aligned} V_{n\,j} = -V_\infty\left(\sin\alpha\cos\beta_j - \cos\alpha\sin\beta_j\right) + \left(w^{(1)}_{GL\,j1}\cos\beta_j - u^{(1)}_{GL\,j1}\sin\beta_j\right)\gamma_1 + \\ + \sum_{i=2}^{N}\left[\left(w^{(1)}_{GR\,j,i-1} + w^{(1)}_{GL\,ji}\right)\cos\beta_j - \left(u^{(1)}_{GR\,j,i-1} + u^{(1)}_{GL\,ji}\right)\sin\beta_j\right]\gamma_i + \\ + \left(w^{(1)}_{GR\,jN}\cos\beta_j - u^{(1)}_{GR\,jN}\sin\beta_j\right)\gamma_{N+1} = 0; \qquad i,j = 1...N. \end{aligned} \tag{2.22}$$

The form of the boundary condition results from fact that left-hand side value of circulation strength for the current panel number $i$ must be equal to the right-hand side value of circulation strength for panel number $i-1$ The condition results from continuity of vorticity distribution over airfoil surface (Fig. 3) This is valid for panels with numbers ranging from 2 to $N$. Because the boundary condition may be written for $N$ panels, expression (2.22) represents a system of $N$ linear equations with $N+1$ unknowns.

To close the system, one applies a Kutta-Joukovski condition. For the purpose of calculations presented below, it was assumed that trailing edge corresponds to stagnation point[2]

$$\gamma_1 + \gamma_{N+1} = 0. \tag{2.23}$$

Now, the influence coefficients take form:

$$\begin{aligned} a_{j1} &= w^{(1)}_{GL\,j1}\cos\beta_j - u^{(1)}_{GL\,j1}\sin\beta_j, && j = 1...N \\ a_{j,N+1} &= w^{(1)}_{GR\,jN}\cos\beta_j - u^{(1)}_{GR\,jN}\sin\beta_j, && j = 1...N, \\ a_{ji} &= \left(w^{(1)}_{GR\,j,i-1} + w^{(1)}_{GL\,ji}\right)\cos\beta_j - \left(u^{(1)}_{GR\,j,i-1} + u^{(1)}_{GL\,ji}\right)\sin\beta_j, && j = 2...N, \\ a_{N+1,1} &= 1, \\ a_{N+1,i} &= 0, && i = 2...N, \\ a_{N+1,N+1} &= 1. \end{aligned} \tag{2.24}$$

[2] There is not the only possible form of Kutta-Joukowski condition. One may find a review of this conditions for example in [16].

Note that the influence coefficients for the first $N$ equations are normal components of velocities induced by unit strength vorticity distribution $\gamma_i=1$ at collocation point number $j$.
The right hand side vector is given by:

$$b_j = V_\infty \left(\sin\alpha \sin\beta_j - \cos\alpha \sin\beta_j\right), \qquad j = 1...N, \qquad b_{N+1} = 0. \tag{2.25}$$

Now, one may complete the set of $N+1$ equations with $N+1$ unknowns.

$$\sum_{i=1}^{N+1} a_{ji}\gamma_i = b_j \quad \text{for} \quad i = 1...N+1. \tag{2.26.}$$

Step 3: Solution of the linear system of equations (2.26.)
The solution may be obtained by standard methods of linear algebra.

Step 4: Determination of velocities and pressure distributions
Once the solution is obtained one may calculate velocity distribution on the airfoil. It could be done by equating strength of the vortices at the corners of the panels (nodes) to the tangential velocity:

$$V_{ij} = \begin{cases} \gamma_j & \text{for} \quad j = 2,...,N, \\ 0 & \text{for} \quad j = 1,...,N+1. \end{cases} \tag{2.27}$$

In the present approach, the velocity is calculated exactly *at the surface* of the airfoil (see Fig. 12) Hence, there is no need to find tangential velocity in such a form as in the method presented, for example, by J. Katz and A. Plotkin in [9], where the velocity is calculated by projection of components of inflow and induced velocity on tangential direction in the collocation point. When the surface velocity distribution is known, the pressure coefficient may be calculated from formula

$$\Delta C_{p_j} = 1 - \left(V_{ij}/V_\infty\right)^2. \tag{2.28}$$

## 3. Numerical results

In this section, a results of numerical calculations will be shown. The first example shows solution for a circular cylinder with no circulation. Calculations were done for the number of panels as low as 8, 12, and 24, and then compared with well-known exact solution for circular cylinder. The results are presented at Fig. 4. The maximum error is shown in Table 1.

Table 1.

| Number of panels | Max. error of velocity % |
|---|---|
| 8 | 0.381 |
| 12 | 0.129 |
| 24 | 0.073 |

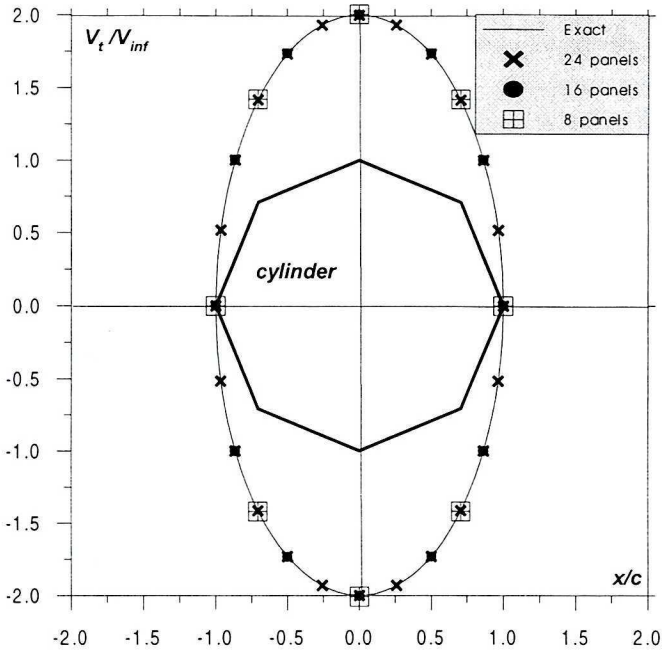


Fig. 4. Comparison of exact solution for circular cylinder with SVM results

As one may see, there is an astonishingly good agreement between analytical and numerical solution even for the number of panels as low as eight. The next solution shows (Fig. 5) results obtained for symmetrical airfoil *NACA 0012* for

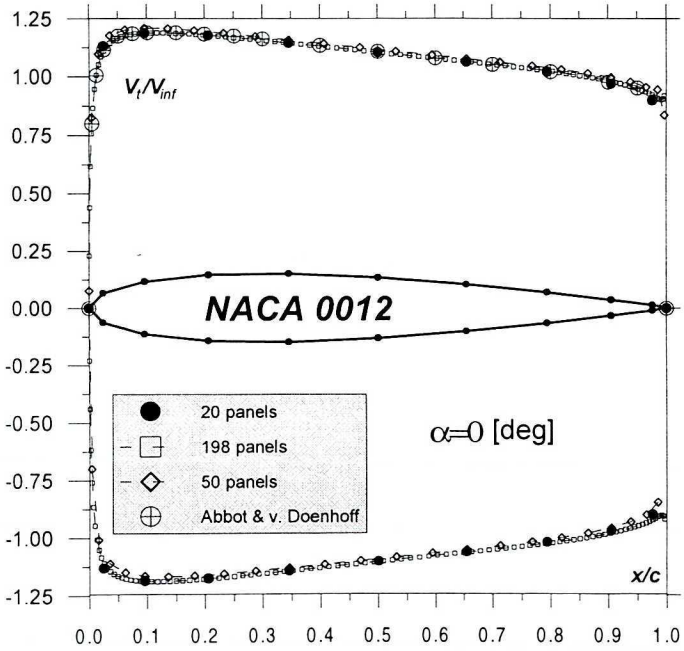


Fig. 5. Comparison of SVM for various numbers of panels for NACA 0012 airfoil (1)

20, *50* and *198* panels compared with theoretical velocity distribution based on conformal mapping method given in [1].

Ain this figure a coarse grid (*20* panels) is also depicted. The results show again good agreement even for *20* boundary elements. The next example (Fig. 6) depicts the velocity over the same airfoil, for number of panels ranging from *10* to *25*. Even for a such small number of panels as *10*, one may find a good agreement between the results of calculations and the data from [1] Fig. 7 shows results for the same airfoil at angle the of attack $\alpha=4.0$ [°]. The difference between results obtained for different grids are negligible except of $N=198$ where the influence of small, but finite trailing edge radius results in peak in velocity distribution for points $j=2$ and $j=197$.

The next example shows results for laminar symmetrical airfoil NACA 63 $_3$ – 018. The airfoil has cusped trailing edge, and velocity at trailing edge has non-zero value (the case of so-called "loaded" t.e.) However, with exception of the trailing edge point, the velocity distribution agrees very well with that given in [1] for symmetrical inflow as well as for design lift coefficient $C_{Ld}=0.32$.

It is worth to note that the coordinates of ends of panels in the analysed case corresponded to the ones from [1], except of two points added at leading edge. This was done for a better description of leading edge curvature. This discrepancy between velocity distributions is caused by the assumed form of Kutta-Joukowski condition (2.23.), which is equivalent to placing a stagnation point at trailing edge of the airfoil.

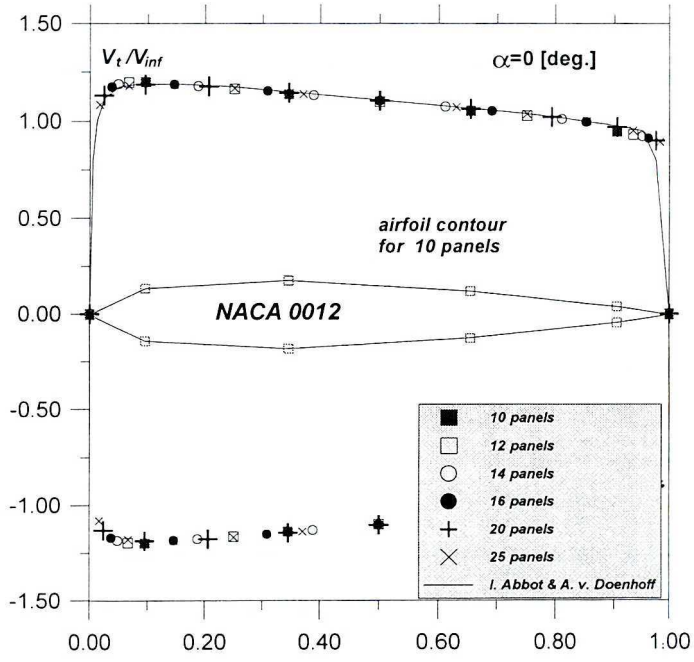


Fig. 6. Comparison of SVM for various numbers of panels for NACA 0012 airfoil (2)

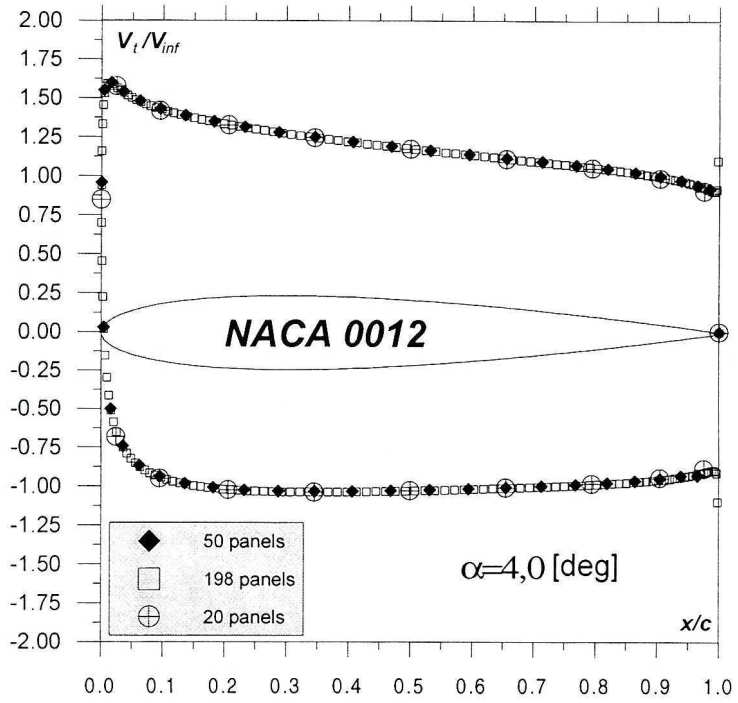


Fig. 7. Comparison of SVM for various numbers of panels for NACA 0012 airfoil (3)

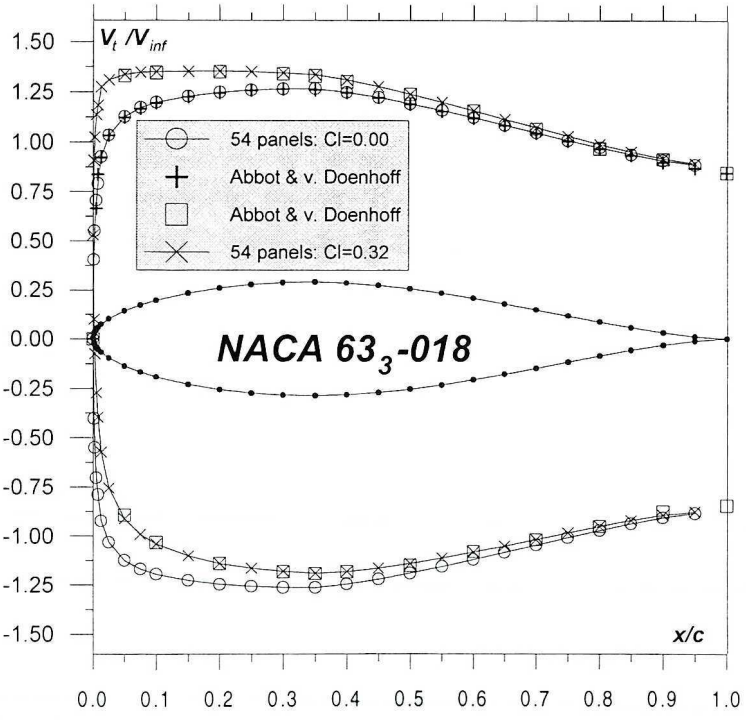


Fig. 8. Comparison of SVM with conformal mapping solution [1] for NACA $63_3$-018 airfoil

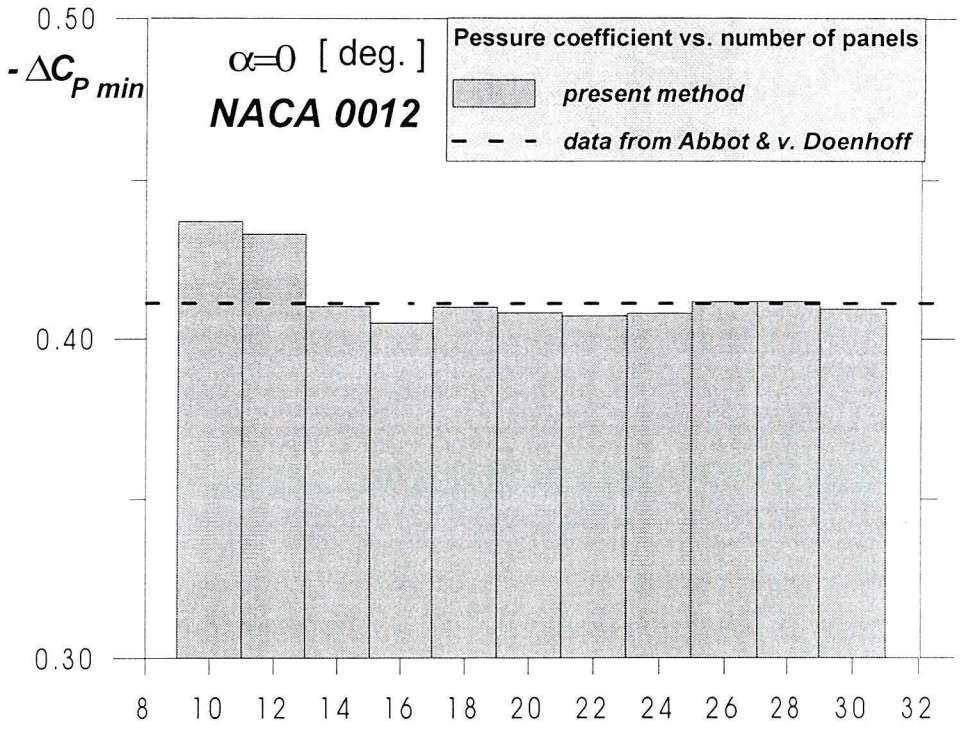


Fig. 9. Influence of the number of panels on $\Delta C_{pmin}$ for NACA 0012 airfoil

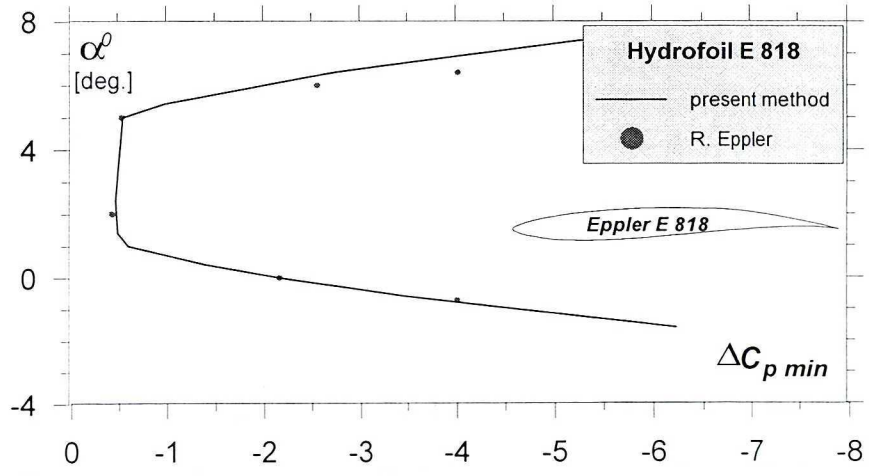


Fig. 10. Minimum pressure coefficient as a function of angle of attack. Calculations for E 818 9,35% thick hydrofoil. *64* panels

The next example, shown in figure 9, illustrates influence of the number of panels on calculated value of minimum pressure coefficient. One may see that number of panels exceeding $N=20$ gives sufficient accuracy of the value of minimum pressure on the airfoil.

Figure 10, shows the minimum pressure coefficient as a function of incidence. Calculations are done conducted for *9,35%* thick hydrofoil E 818 The angle of attack is measured from zero lift angle. For this hydrofoil, zero lift angle is equal to $\alpha_0 = -4.42$ [deg]. The results are compared with available data, presented in [6] The calculations were done for hydrofoil contour coordinates given in [6]. The predicted behaviour of $\Delta C_{pmin}$ versus angle of attack, shows very good agreement with experimental data.

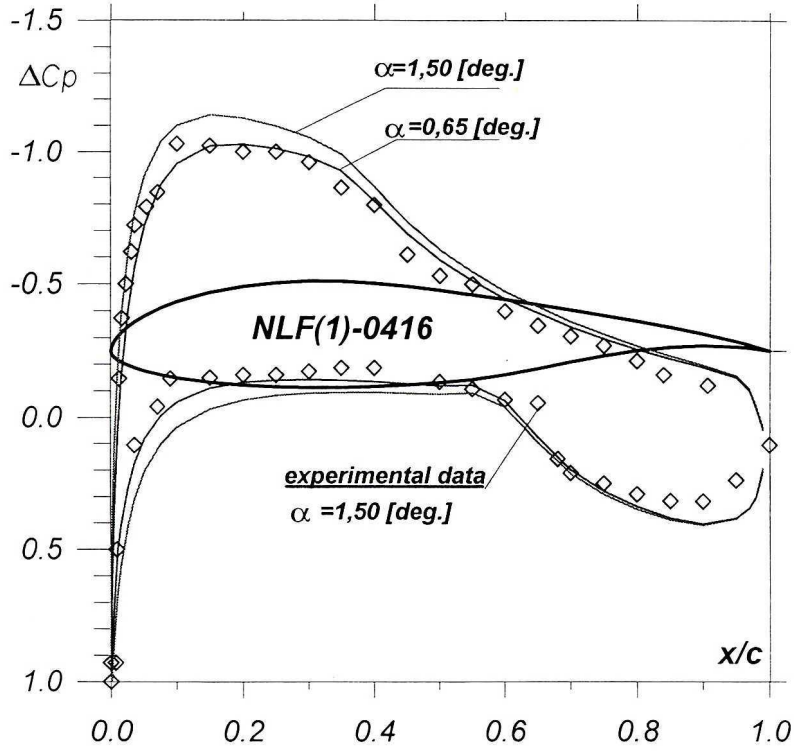


Fig. 11. Comparison of calculated and measured [14] pressure distributions for wind turbine airfoil NLF(1)-0416. Number of panels: *64*

It is worth to note that the accurate prediction of minimum pressure coefficient is very important in aviation technology. It makes it possible to predict a critical Mach number from incompressible flow calculation It is also applicable to marine engineering, because it facilitates proper estimation of the beginning of cavitation.

The last example shows comparison between experimental pressure data and pressure distribution obtained by the presented method. The experimental data

were obtained [14] at Reynolds number $Re=1\cdot10^6$. The pressure distributions are in a good agreement with experimental data for angle of attack $\alpha=1,50$ [deg]. However, the numerical results fit better to the experimental data for angle the of attack equal *0,65* [deg] accepted in the calculations. This discrepancy may be a result of the uncertainty of measurement of the angle of attack, as well as model geometry (the theoretical contour of the airfoil was used to the calculations).

## 4. Conclusions and final remarks

The outlined approach to calculation of tangential velocities over airfoil surfaces, based on Martensen's interpretation of surface vorticity distribution allows us to get a better quality of numerical solution in comparison with the results presented in [9] the order of the number of panels given by Katz and Plotkin to obtain satisfactory results for linear vortex distribution method was about *100*.

The presented approach to the problem leads also to simplification of the numerical code, because once the system of equations for vorticity distribution is solved, the values of tangential velocity are also known. Another advantage offered by the presented method of calculation of velocity and pressure consists in the fact, that one obtains velocity at the *real* contour of the airfoil, Fig. 12.
In the case of conventional panel methods, the velocity is calculated in the mid-point of the panel (collocation point), which lays inside or outside of the given contour of airfoil. One should note that calculation of the tangential velocity in grid nodes is also employed in potential based panel methods [9]. However, this requires numerical differentiation of velocity potential, which might lead to the numerical errors.

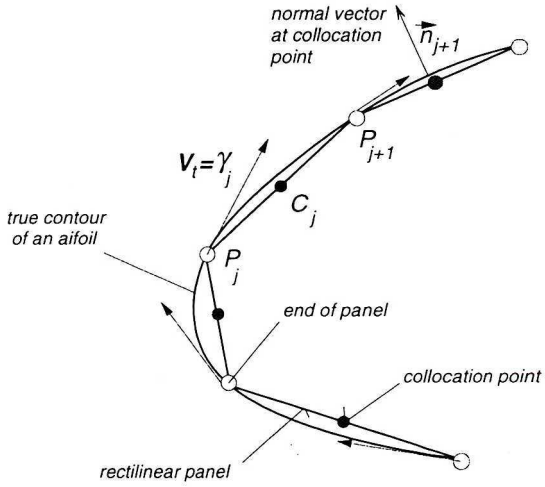


Fig. 12. Tangential velocity at grid points. Schematic

The comparison between velocity and pressure distributions based on theoretical (Figs. 4÷9) and experimental (Figs 10 and 11) data show good agreement. The influence of the number of boundary elements on minimum pressure distribution has also been investigated. This quantity is specially important, because it allows for prediction of critical Mach number from incompressible flow calculations (aviation technology), as well as for the prediction of cavitation (marine engineering). It also can be treated as a measure of accuracy of pressure prediction. The number of panels $N=20$ gives sufficient accuracy of the value of minimum pressure on the airfoil. For rough estimate of velocity distribution, even lower number of panels would be sufficient (see: Figs. 4, 6 and 7) This allows us to do calculations even by means of a programmable calculator.

Manuscript received by Editorial Board, March 14, 2001;
final version, February 12, 2002.

## REFERENCES

[1] Abbot I. H., von Doenhoff A. F.: Theory of Wing Sections. Dover Publ., 1959.

[2] Babah M.: Study of the influence of different parameters on the numerical solution of the panel method for solving incompressible potential flow around multi-element airfoils. PhD Thesis, Poznań University of Technology, Dept of Mechanical Engineering 1997.

[3] Belotserkovskii S.M. et al.: Matematicheskoye Modielirovanije Ploskoparaliel'novo Obtiekanija Tiel. Izd. „Nauka", Moskow 1988 (in Russian).

[4] Chiu T. W.: A two-dimensional second-order votex panel method for the flow in a cross-wind at large yaw angles up to 90 degrees. Journal of Wind Engineering and Industrial Aerodynamics No. 45 (1992), pp. 47÷74.

[5] Coullite C., Plotkin A.: Aerofoil Ground Effect Revisited. Aeronaut. J. 100 (992) 1996, pp. 65÷74.

[6] Eppler R.: Airfoil Design and Data. Springer Verlag 1990.

[7] Goraj Z., Pietrucha J.: Modified Panel Methods with Examples of applications to Unsteady and Non-linear Flow Field Calculations. Transactions of The Institute of Aviation, No 152, 1/98, pp.41÷60.

[8] Goraj Z., Sznajder J.: Panel Methods in Flight Mechanics-Possibilities and Limitations. Transactions of The Institute of Aviation, No 143, 1/95, pp. 59÷102.

[9] Katz J., Plotkin A.: Low-Speed Aerodynamics. From Wing Theory to Panel Methods. McGraw-Hill Inc., 1991, pp. 316÷359.

[10] Martensen E.: Die Abrechung der druckverteilung am Dicken Glitterprofilen mit hilfe von Fredholmschen Integralglaichungen. Zweiter Art. Arch. Ret. Mech. Anal. 3, 1959 pp. 235÷237.

[11] Meric R. A.: Boundary Elements and Optimization for Linearized Compressible Flows Around Immersed Airfoils. Engineering Analysis with Boundary Elements, No. 23 (1999), pp. 591÷596.

[12] Rohatyński R.: Method of Boundary Elements in Fluid Mechanics. Transactions of The Institute of Aviation 2/1996, pp. 136÷144.

[13] Sorko S. A.: The Application of the Integral Equation For Determination of 2-D and 3-D Flows of Perfect Fluid. Transactions of The Institute of Aviation 2/1996, pp. 164÷195 (in Polish).

[14] Späth M., Brand A.J.: Field Rotor Aerodynamics with Vortex Generators. Second European Fluid Mechanics Conference, September 20–24, 1994, Warsaw, Poland.

[15] Stalewski W.: Numerical Analysis of Perfect Fluid Flow Around of an Airfoil. Transactions of The Institute of Aviation, No. 112–113, 1988, pp. 61÷74 (in Polish).

[16] Xu C.: Surface Vorticity modeling of flow around airfoils. Computational Mechanics, No. 21 (1998), pp. 526÷532.

[17] Xu C., Yeung W. W. H.: Discrete Vortex Method for Airfoil With Unsteady Separated Flow. Journal of Aircraft, Vol. 33, No. 6, 1996, pp. 1208÷12010.

## O pewnej metodzie wyznaczania rozkładów prędkości w metodzie panelowej wykorzystującej ciągły rozkład wirów

Streszczenie

W pracy przedstawiono zastosowanie interpretacji ciągłego rozkładu wirowości na powierzchni profilu podanej przez E. Martensena w celu uproszczenia obliczeń rozkładów prędkości w płaskim przepływie potencjalnym. Dla celów obliczeniowych wykorzystano metodę panelową z liniowym rozkładem natężenia cyrkulacji wzdłuż panelu, z warunkiem brzegowym Neumana i warunkiem Kutty-Żukowskiego równoważnym umiejscowieniu punktu spiętrzenia na krawędzi spływu.

W artykule przedstawiono również szczegółowo użytą procedurę numeryczną. Główną różnicą pomiędzy spotykanymi dotąd realizacjami metody wykorzystującej powierzchniowy rozkład wirów (SVM) jest wyznaczanie prędkości stycznych nie w punktach kolokacji, a w narożach wielokąta aproksymującego profil. Powyższe podejście pozwala na redukcję kosztu obliczeniowego metody SVM, dzięki możliwości zastosowania stosunkowo niewielkiej liczby paneli, przy poprawie jakości rozwiązania. Dodatkową korzyścią jest, iż rozwiązanie otrzymuje się na rzeczywistej powierzchni profilu, a nie w punktach kolokacji, leżących (zależnie od lokalnej krzywizny profilu) wewnątrz lub na zewnątrz konturu.

W pracy przedstawiono wyniki obliczeń numerycznych ilustrujące zastosowanie opisywanej metody. Wyniki porównano z zarówno ze znanymi wynikami teoretycznymi jak i danymi doświadczalnymi. Uzyskano dobrą zgodność rozkładów prędkości i ciśnień na powierzchni wybranych profili. W dwóch przykładach służących za ilustrację prezentowanej metody uzyskano dobrą zgodność rozkładów prędkości nawet w przypadku tak niskiej liczby paneli jak dziesięć. Ta ostatnia okoliczność pozwala na zastosowanie opisanego tu podejścia do wykonywania zgrubnych obliczeń rozkładów prędkości, nawet przy pomocy kalkulatora programowanego.